A Fiber Optic/Millimeter-Wave Radio Transmission Link Using HBT as Direct Photodetector and an Optoelectronic Upconverter

Eiji Suematsu, *Associate Member, IEEE,* Nobuaki Imai, *Member, IEEE*

Abstract— **The performance of a fiber optic subcarrier link using an HBT as a direct photodetector and an optoelectronic up-converter in 50 GHz band has been experimentally investigated at a wavelength of 0.83 μm. From comparison with the performances of links using other MMIC-compatible photodetectors and with that of a high speed PIN-photodetector, this paper shows that the HBT-photodetector is superior to the other MMIC compatible photodetectors (MSM and HEMT). It is also shown that HBT not only has a high photodetection ability in the millimeter-wave band but also provides low conversion loss between a microwave subcarrier modulated by an optical signal and a millimeter-wave carrier. Also demonstrated are video FM-subcarrier transmission and 140 Mbps QPSK digital radio transmission using an HBT optical/RF transducer. At transducer transmission power of around −20 dBm, the HBT optical/RF transducer allows 50 GHz band radio transmission over optical fiber to achieve a weighted SNR of more than 50 dB and a data rate of 140 Mbps in indoor application.**

I. Introduction

MILLIMETER-WAVE frequencies are very promising RF frequencies for transmitting broadband signals, e.g., video signals and high-speed data, because they can reduce mutual interference and reuse the frequency resources [1], [2]. Previously, broadband video distribution networks have been demonstrated using subcarrier multiplexing techniques that are capable of handling multi-channel analog and/or digital signals [3], [4]. The techniques utilize the advantages of fiber optic subcarrier transmission, which include low transmission loss, potential bandwidth and radio signal compatibility. Fiber optic subcarrier transmission systems are also being investigated as a mean of exploiting the potential of the millimeter-wave band, both for wideband personal radio communication based on a micro/pico-celled system architecture [5]–[7] and for a high-speed millimeter-wave local area network (LAN) [8]. The radio zones above the systems are formed within a range of several meters to a few hundred meters in indoor and outdoor applications. These systems require a large number of optical/RF transducers operating in the millimeter-wave band for signal radiation or distribution. They also require optical components operating in the millimeter-wave band. It is thus very important to develop cost-effective and compact optical/millimeter-wave transducers. However, with commercially available optical components [e.g., laser diodes (LD's), external optical modulators (EOM's) and photodiodes], there are frequency limits of less than 8 GHz and 20 GHz at wavelengths of 0.8 μm and 1.3–1.55 μm bands, respectively. This paper investigates the optical fiber/millimeter-wave radio link and proposes a cost-effective and compact optical fiber/RF transmission system that uses commercially available optical components (EOM and LD) and an HBT-photodetector.

To realize these systems, optoelectronic integrated circuit (OEIC) technology is another alternative for compact and inexpensive hardware. However, despite many potential advantages of monolithic integration, the OEIC's have yet to outperform hybrid integrated circuits because of their complicated fabrication process and inherent circuit limitations [9], [10]. Furthermore, these systems differ from an ultrawideband (DC to microwave) optical fiber communication system using OEIC's in that they involve millimeter-wave band radio transmission after photodetection, and hence, require such millimeter-wave components as a low-noise amplifier, a high-power amplifier, a filter, and an antenna for the radio transmission. An MMIC-compatible optical device is thus the best alternative for an optical/RF transducer module.

MMIC compatible devices are classified into two groups: two-terminal devices (diodes) and three terminal devices (transistors). The main type of the first group is the metal-semiconductor-metal photodetector (MSM-PD) [11], [12]. The second group is represented by heterojunction phototransistor (HPT) [13], [14], MESFET [17]–[19], HEMT [5], [20]–[23], and HBT [23]–[25]. The MSM-PD has demonstrated a 3-dB bandwidth of more than 100 GHz [12]. The MSM-PD, however, has a low responsivity and significant trade-off among responsivity, bandwidth, and driving voltage. The HPT's used as two- or three-terminal devices have a structure similar to that of the HBT's [13]–[16]. The operation frequency of the HPT is less than a few hundred MHz because of its circular emitter, which has a diameter that exceeds 10 μm [13], [14]. On the other hand, MESFET, HEMT, and HBT, as basic three-terminal MMIC-building blocks, are typically used as photodetectors. These devices also perform the function of optoelectronic mixing [19], [26].

The optoelectronic mixing frequency-mixes the photocurrent signal in the photodetector with a local oscillator signal

Manuscript received April 10, 1995; revised October 2, 1995.

E. Suematsu was with ATR Optical and Radio Communications Research Laboratories, 2-2 Hikaridai, Seika-cho, Soraku-gun, Kyoto 619-02, Japan. He is now with Central Research Laboratories, SHARP Corporation, 2613-1 Ichinomoto-cho, Tenri, Nara 632, Japan.

N. Imai is with the ATR Optical and Radio Communications Research Laboratories, 2-2 Hikaridai, Seika-cho, Soraku-gun, Kyoto 619-02, Japan.

Publisher Item Identifier S 0018-9480(96)-00470-X.

TABLE I
SUMMARY AND ABBREVIATIONS OF MMIC COMPATIBLE PHOTODETECTORS

Photodetectors			Direct Photodetection	Optoelectronic Upconversion
MMIC Compatible	3-Terminal	HBT	HBT-DD	HBT-OUP
		HEMT (FET)	HEMT-PD	Not Studied
	2-Terminal	MSM	MSM-PD	----------
MMIC Uncompatible		PIN	PIN-PD	----------

(LO) by using the inherent nonlinearlities in the device. It is suitable for three terminal photodetectors because the mixer requires a three port terminal for LO-, IF-, and RF-signals. On the other hand, in the above systems, the required bandwidth is in the range of several-hundred MHz to a few GHz; accordingly, optical fiber transmission does not require the use of a millimeter-wave subcarrier. Therefore, if a photoreceiver that functions as an up-converter allows a microwave subcarrier of a few GHz to be converted to a millimeter-wave carrier, the optical components can be optimized with respect to performance and cost. Moreover, three terminal devices such as the optoelectronic mixer (upconverter) not only meet this requirement but can also realize a compact, simple, and cost-effective MMIC optical/RF transducer in the millimeter-wave band.

The aim of this paper is to experimentally study GaAs-HBT photodetectors, which have two kinds of photodetection functions, i.e., HBT direct photodetector (HBT-DD) and optoelectronic upconverter (HBT-OUP) at 0.83 μm wavelength. Table I summarizes the MMIC compatible photodetectors studied in this paper. This paper also proposes millimeter-wave radio transmission systems using the HBT photodetector over an optical fiber link. Section II describes the fiber optic subcarrier link performance while using the HBT-DD and HBT-OUP links with respect to frequency response and signal (subcarrier)-to-noise ratio (SNR). Section III demonstrates the application of an optical fiber/radio link for a 50 GHz band video FM-subcarrier transmission and 140 Mbps QPSK digital radio transmission systems. Section IV discusses the transmission forms using the HBT-DD and HBT-OUP links.

II. FIBER OPTIC SUBCARRIER LINK PERFORMANCE

The system concept of an optical fiber/millimeter-wave radio link for personal radio communication is shown in Fig. 1. In the central base station, optical carriers are intensity-modulated by the millimeter-wave subcarrier multiplexing signal. They are transmitted by single mode fiber and then converted into millimeter-wave carriers by the optical/RF transducer with an HBT photodetector and an MMIC transmitter. The millimeter-wave carriers are subsequently radiated over the microcell zone and received by wireless multimedia terminals on a liquid crystal display.

Fig. 2 shows a block diagram of the above-mentioned system, which is composed of the optical fiber transmission link as the first stage and the millimeter-wave transmission

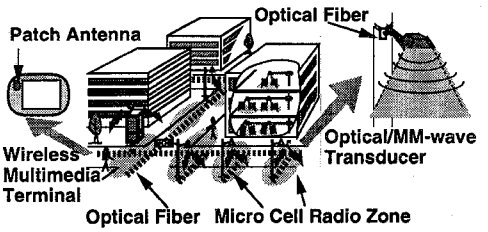

Fig. 1. System concept of optical fiber/millimeter-wave radio link for personal radio communication.

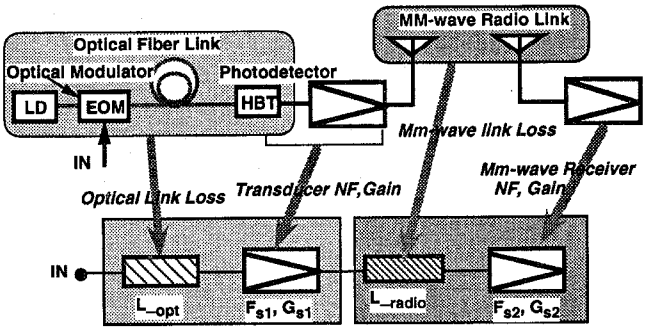

Fig. 2. Block diagram of optical fiber/millimeter-wave radio link (down link).

link as the second stage. When relative intensity noise (RIN) of the LD is small or even negligible, the total noise figure of the link, F_t, is given as follows

$$F_t = L_{opt} \cdot F_{s1} + \frac{L_{radio} \cdot F_{s2} - 1}{\frac{G_{s1}}{L_{opt}}} \tag{1}$$

where L_{opt} is optical link loss between the optical modulator's input subcarrier signal and the photodetector's output signal, L_{radio} is millimeter-wave radio channel loss, F_{s1} and F_{s2} are the noise figures of the transducer and millimeter-wave receiver, respectively, and G_{s1} is the gain of the transducer. If $(G_{s1}/L_{opt}) \gg 1$, F_t mainly depends on the optical link loss L_{opt}. On the other hand, if $(G_{s1}/L_{opt}) \leq 1$, F_t depends on all of the parameters, including L_{opt}, F_{s1}, L_{radio}, and F_{s2}. In both cases, optical link loss L_{opt}, transducer noise figure F_{s1}, and gain G_{s1} are important parameters governing link performance.

A. Link Configurations

Fig. 3 shows the fiber optic subcarrier link configuration and experimental setup for photodetector characterization. The fiber optic millimeter-wave subcarrier direct detection links consist of LD, EOM, optical fiber, and HBT-DD or other photodetectors (Fig. 3(a)). The IF subcarrier up-converter link is composed of an LD, EOM, optical fiber, HBT-OUP, and local oscillator (Fig. 3(b)). These configurations use a Mach–Zehnder Z-cut $LiNbO_3$ EOM with a 3-dB bandwidth of 5 GHz because the LD's direct modulation is usually limited to frequencies below its relaxation oscillation frequency (typically <8 GHz for high-speed commercially available devices in 0.8 μm wavelength band). Conversely, the EOM used in the configuration is capable of modulation into the

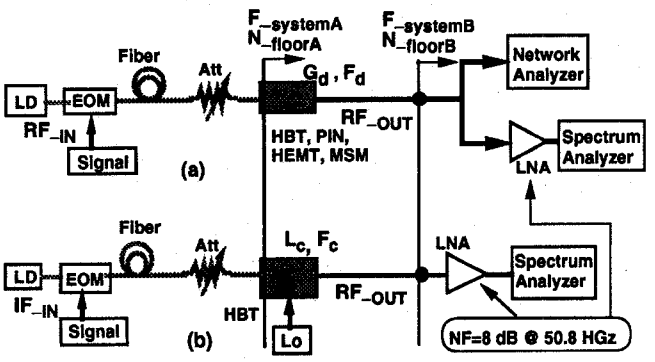

Fig. 3. Link configuration and experimental setup for frequency response and SNR (subcarrier-to-noise ratio) measurements of (a) HBT-DD or PIN-PD (direct detection links) and (b) HBT-OUP (optoelectronic up-converter) link. The IF or RF power input to the EOM is 0 dBm.

millimeter-wave band. This is because it does not suffer the characteristic roll-off due to the relaxation oscillation frequency of the LD at high frequency.

B. Frequency Response of MMIC Compatible Photodetectors

At a 0.83 μm wavelength, MMIC compatible photodetectors (i.e., MSM-PD, HEMT-PD, and HBT-DD) are characterized by their use of a modified electro-optic, on-wafer RF probe station and network analyzer [5], [22]–[25] (Fig. 3(a)).

The schematic configurations of the MMIC compatible photodetectors are shown in Fig. 4. When light is incident on the electrodes of the HBT, the photon is absorbed into the gaps among the emitter-, base-, and collector electrodes. Electron hole pairs are generated in the base-collector junction. The photogenerated current acts as the base current for the input signal. The area of the HBT electrodes, i.e., 3 μm $\times$ 20 μm $\times$ 1 emitter, is roughly the same as the optical beam-spot area of $\leq$15 μm. The HBT has an $f_{\max}$ of 32 GHz under dc-operating conditions of $V_{CE} = 4$ V, $I_C = 12$ mA [27]. The MSM-PD and HEMT-PD were fabricated on the same wafer by the MMIC GaAs-HEMT fabrication process. The HEMT, which has a maximum oscillation frequency $f_{\max}$ of 50 GHz, has a gate length of 0.3 μm and a gate width of 25 μm $\times$ 2 [5], [22], [23]. The MSM was fabricated on a 1 μm undoped GaAs MBE-grown buffer layer. The Schottky contact is fabricated in the same manner as the gate metal of the recessed-gate HEMT. The active area of the diode is 14 μm $\times$ 12 μm, and it contains 0.3 μm $\times$ 20 μm $\times$ 4 fingers with 1 $\times\mu$m spacing. The area is the same as that of the optical beam spot. The driving voltage of the MSM is 10 V. The HBT and HEMT are discrete devices having a common emitter and a common source configuration, respectively.

Fig. 5(a) and (b) show the measured insertion loss (link gain) between the EOM's input and the photodetector's output. The 0 dB reference plane is RF_IN and IF_IN in Fig. 3. For reference, this figure also shows a PIN-PD with a 3-dB bandwidth of 40 GHz and dc-responsivity of 0.11 A/W at a 0.83 μm wavelength. The link losses include the EOM response with a 3-dB bandwidth of 5 GHz and an optical insertion loss of 7 dB. In the microwave band, the HBT has a higher link gain than the other MMIC compatible photodetectors and the

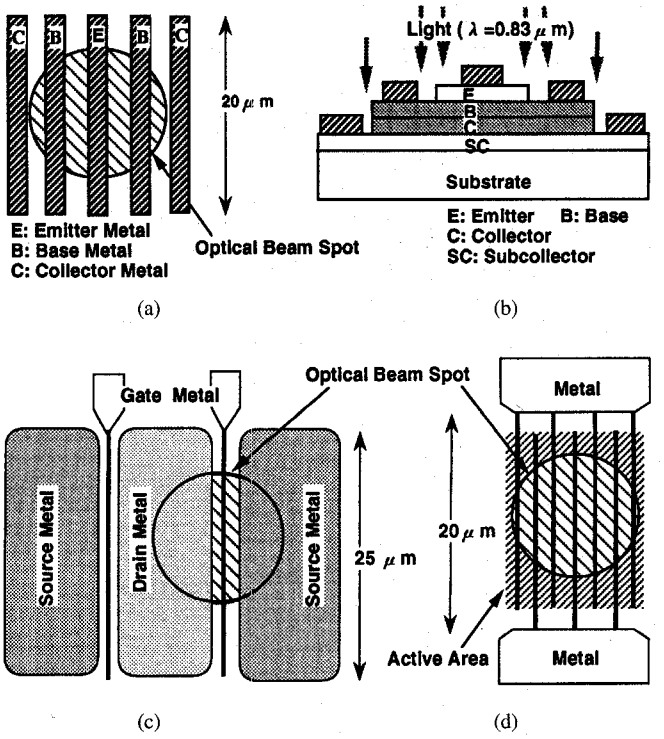

Fig. 4. Schematic configuration of MMIC compatible photodetectors: (a) top view of HBT, (b) cross-sectional view of HBT, (c) top view of HEMT, and (d) top view of MSM-Photodetector.

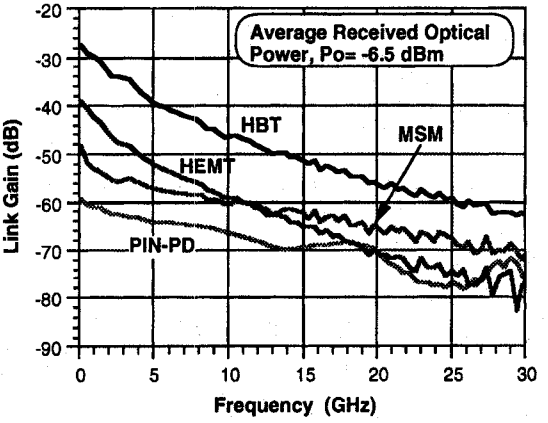

Fig. 5. Measured link gain (a) between EOM input port and MMIC compatible photodetector output port, and between EOM input port and PIN-PD output port. The f_3 dB and dc-responsivity of PIN-PD are 40 GHz and 0.11 A/W, respectively. The bias conditions of HBT-DD are $V_{CE} = 4$ V, $I_B = 70$ uA ($I_C = 12$ mA), and those of HEMT and MSM and PIN-PD are $V_{DS} = 2$ V, $V_{GS} = 0$ V ($I_D = 17$ mA), $V_{MSM} = 10$ V, and $V_{PIN} = 9$ V, respectively.

PIN photodetector because of its internal gain and high optical coupling efficiency. The lower link loss (higher link gain) is essential for decreasing the total link noise figure F_t (1). The HBT photoresponsivity curves loosely depend on the S_{21} small-signal gain [24], [25]. The optical coupling efficiency, i.e., the quantum efficiency of the photodiode formed by the base-collector junction of the HBT-DD, is in the range of 30–40%, depending on the electrode configuration and optical beam spot [24], [25].

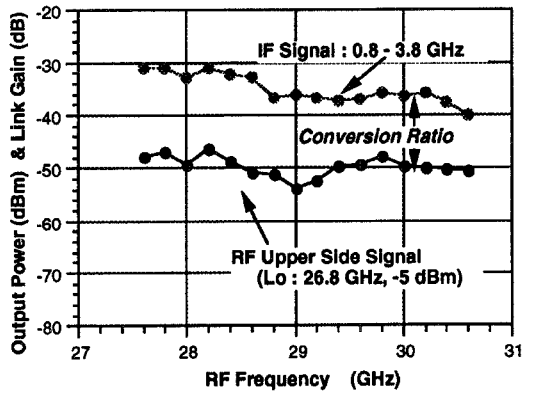

(a)

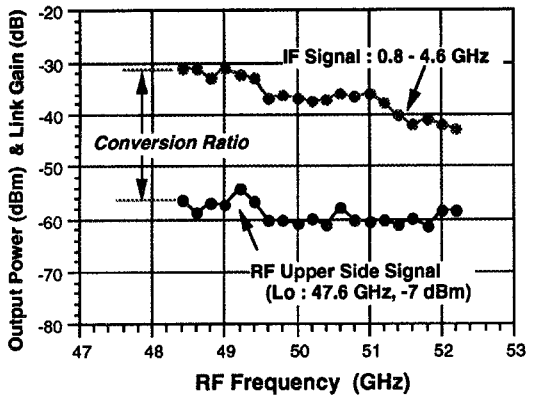

(b)

Fig. 6. Frequency response of detected IF signal and RF upper side signal of HBT-OUP (optoeletronic upconverter): (a) at IF = 0.8–3.8 GHz/RF = 27.6–30.6 GHz and (b) at IF = 0.8–4.6 GHz/RF = 48.4–52.2 GHz. The IF power input to EOM and received average optical power are 0 dBm and −6 dBm, respectively. The bias conditions of the HBT-OUP are V_{CE} = 4 V, V_{BE} = 1.3 0 V (I_C = 2.6 mA).

C. Frequency Response of HBT-OUP

Fig. 6(a) and (b) show the IF and RF (upper sideband) frequency response of the HBT-OUP, which is converted by a local oscillator signal supplied to the HBT base terminal. The conversion ratios, i.e., the power differences between the IF- and RF-detected power at the HBT output port, are 13 dB at IF = 3.2 GHz/RF = 30 GHz and 23 dB at IF = 3.2 GHz/RF = 50.8 GHz. The detected RF (50 GHz and 30 GHz band) signals have a flatter response than the IF signal. The RF signals fluctuate weakly with the IF signal, which is not completely terminated. The HBT has an S_{21} small-signal gain of about 9 dB under the mixer operating conditions V_{CE} = 4 V, V_{BE} = 1.30 V, and I_C = 2.6 mA at 3.2 GHz. Since the detected IF signal includes the 9 dB of S_{21} gain, the estimated conversion losses are about 4 dB at IF = 3.2 GHz/RF = 30 GHz and about 14 dB at IF = 3.2 GHz/RF = 50.8 GHz. At IF = 3.2 GHz/RF = 50.8 GHz, the supplied local power to the HBT was so small that the conversion loss could not be saturated. As a result, the HBT-OUP shows a large conversion loss of 14 dB. The HBT-OUP can also be considered a device that functions as a photodetector, an IF amplifier and a mixer.

D. Noise Performance of the HBT-DD and HBT-OUP in the Millimeter-Wave Band

The experimental setup measures SNR by using a low-noise amplifier and a spectrum analyzer (Fig. 3(a) and (b)). Input RF power to the EOM is 0 dBm. The SNR values were compared among three types of links: a PIN-PD link and HBT-DD links and a HBT-OUP link (Fig. 3(a) and (b)). A low-noise amplifier (LNA) was inserted between these photoreceivers and the spectrum analyzer in order to decrease the noise figure of the spectrum analyzer. The system noise figure $F_{\_systemB}$, seen from the input port of the amplifier, is 8 dB at 50.8 GHz. The gain of the LNA is subtracted from the output (signal and noise) power of the photodetectors.

Under conditions of small average optical power, where there is no effect of the LD's RIN nor any effect of the local oscillator phase noise, the system noise floor $N_{\_floorA}$ seen from the input port of the detector is given as

$$N_{\_floorA}\,(\text{dBm/Hz}) = kT\,(\text{dB}) + F_{\_systemA}\,(\text{dB}) + G_d\,(\text{dB}) \quad (2)$$

$$F_{\_systemA} = F_d + \frac{F_{\_systemB} - 1}{G_d} \quad (3)$$

where $F_{\_systemA}$ are the system noise figures seen from the input port of the detector (Fig. 3), k is Boltzmann's constant, T is temperature, and $kT = -174$ dBm/Hz is the lower limit of the thermal noise floor at room temperature. F_d and G_d are the noise figure and internal gain of the HBT-DD, respectively. On the other hand, if the HBT-DD (and HBT-OUP) have a (conversion) loss and the noise figure is equivalent to the (conversion) loss, the system noise floors $N_{\_floorA}$ seen from input port of the HBT-DD and HBT-OUP, become:

$$N_{\_floorA}\,(\text{dBm/Hz}) = N_{\_floorB}\,(\text{dBm/Hz}). \quad (4)$$

The system noise floors $N_{\_floorA}$ seen from the input port of the HBT-DD and HBT-OUP coincide with the system noise floor $N_{\_floorB}$ seen from input port of the amplifier (Fig. 3).

Fig. 7 show the received average optical power dependence of the detected signal (subcarrier)-to-noise power for the PIN-PD link, HBT-DD link, and HBT-OUP link at 50.8 GHz. The noise floors of the links are composed of the RIN, signal shot noise and receiver noise. As the optical power decreases, the receiver noise gradually becomes dominant. In the HBT-DD and PIN-PD links, the RIN does not affect their noise floors because of the small modulation depth of the EOM due to the large insertion loss of the EOM's electrodes in the 50 GHz band. At an optical power less than −15 dBm (where receiver noise is dominant) in the 50 GHz band, the HBT-OUP link has an SNR 20 dB higher than that of the HBT-DD link and 32 dB higher than that of the PIN-PD link (the PIN-PD link signal is masked by the system noise floor). The noise floor $N_{\_floorA}$ of the HBT-DD link coincides with that of the PIN-PD link because the HBT, with a S_{21} cutoff frequency of 25 GHz, acts as a direct photodetector with no internal-gain (G_d = 0 dB). The noise floors $N_{\_floorA}$ of the HBT-DD, HBT-OUP, and PIN-PD link coincide with the noise floor $N_{\_floorB}$ seen from the input port of the LNA (4).

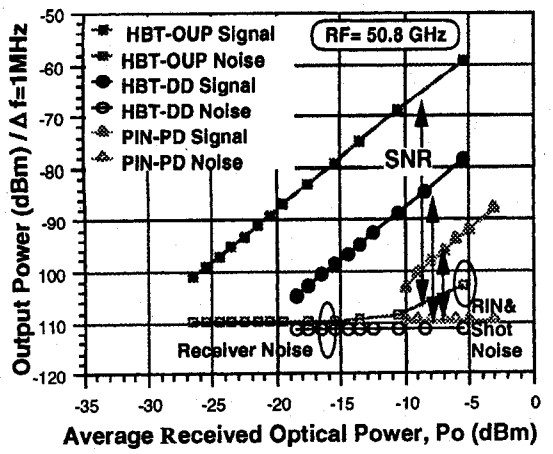

Fig. 7. Received average optical power dependence of detected signal (subcarrier)-to-noise power for HBT-DD link, PIN-PD link at 50.8 GHz, and for HBT-OUP link at IF = 3.2 GHz/RF = 50.8 GHz. The local power supplied to the base terminal of the HBT-OUP is − 7 dBm. The IF and RF power input to the EOM is 0 dBm.

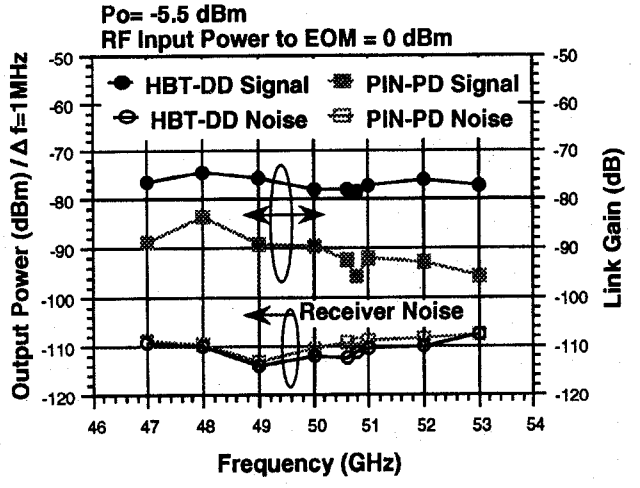

Fig. 8. Frequency dependence of signal (subcarrier)-to-noise power at received optical power of −5.5 dBm. These noise floors are essentially consistent with the system noise figure ($F_{\_systemB}$), which is in the range of 4–10 dB.

Fig. 8 shows the frequency dependence of the signal (subcarrier)-to-noise power for the links when the system noise figure $F_{\_systemB}$ are in the range of 4–10 dB in the 50 GHz band. In the RF bandwidth of 50 ± 3 GHz, the HBT-DD has a flat response due to the S_{21} of 6 dB/octave characteristics [24], [25], and the noise floor of the HBT-DD coincides with that of the PIN-PD, depending on the noise floor of the $F_{\_systemB}$ (4).

Fig. 9 compares the signal (subcarrier)-to-noise power of the HBT-DD link at 3.2 GHz with that of the HBT-OUP link at IF = 3.2 GHz/RF = 50.8 GHz. The HBT-DD has internal gain G_d at 3.2 GHz so that the noise floor $N_{\_floorA}$ of the HBT-DD link depends on the noise performance of the HBT in the small optical power region (2) [25]. The signal level of the HBT-OUP is 23 dB less than that of the HBT-DD at 3.2 GHz. However, above an average optical power P_o of −10 dBm, the noise floor of the HBT-DD at 3.2 GHz rises dramatically due to the increase in the RIN of LD, but that of the HBT-OUP increases slightly, and hence, the SNR of the HBT-OUP link

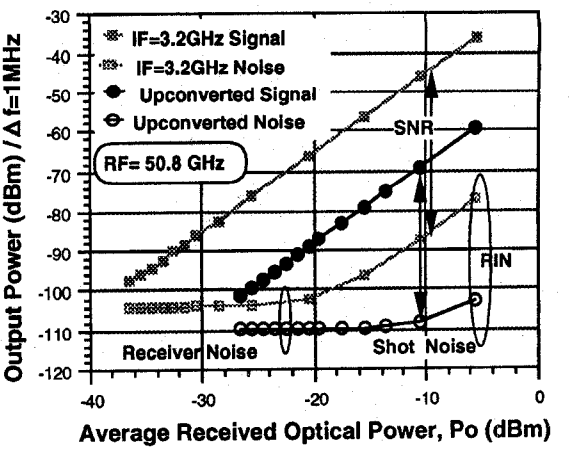

Fig. 9. Received average optical power dependence of detected signal (subcarrier)-to-noise power for HBT-DD link at 3.2 GHz and HBT-OUP at IF = 3.2 GHz/RF = 50.8 GHz.

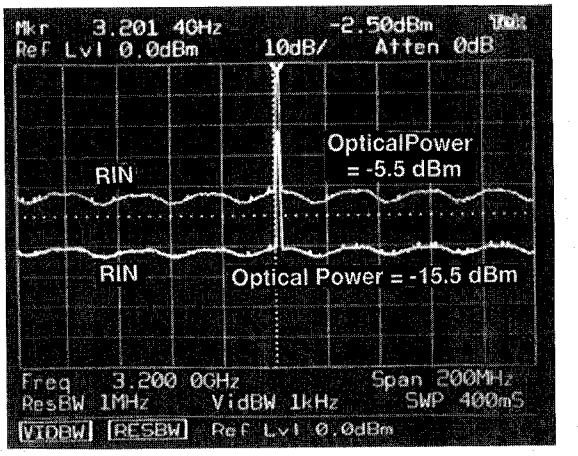

(a)

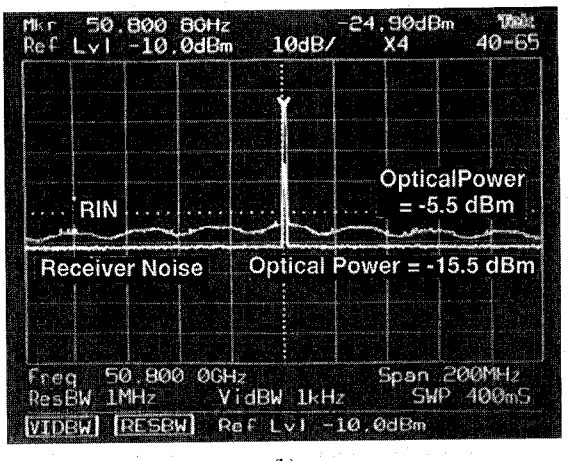

(b)

Fig. 10. (a) HBT-DD's detected IF signals combined with two spectrums at average received optical power of −5.5 dBm and −15.5 dBm. (b) HBT-OUP's upconverted signals combined with two spectrums at average received optical power of −5.5 dBm and −15.5 dBm.

is nearly equal to that of the HBT-DD link at 3.2 GHz. The frequency spectrums of the IF and RF upconverted signals are shown in Fig. 10(a) and (b), respectively. The two spectrums of the received average optical powers of −5.5 dBm and

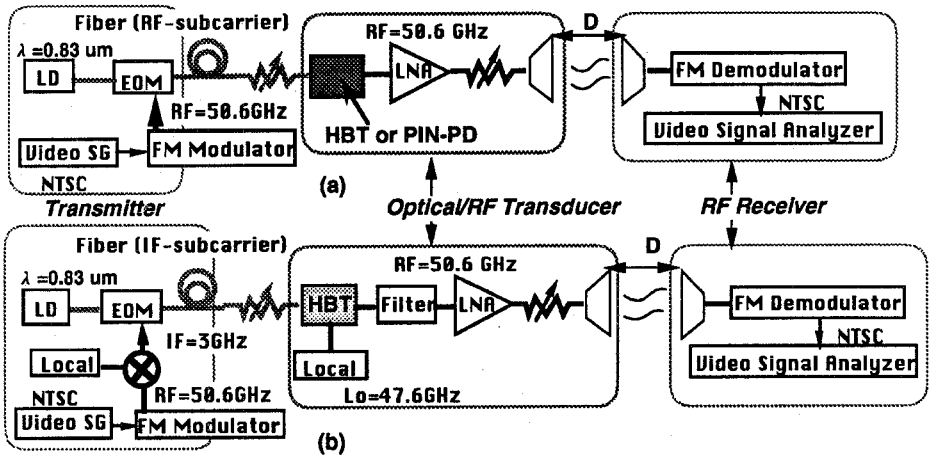

Fig. 11. Experimental configuration of FM-video millimeter-wave transmission link using (a) PIN-PD, HBT-DD, and (b) HBT-OUP link. The HBT-DD and HBT-OUP links in the configurations include the millimeter-wave probe loss of 4.7 dB at 50.6 GHz before LNA.

−15.5 dBm are overwritten in the photograph. As the 10 dB average received optical power increase, the IF spectrums cause the RIN to increase 20 dB (Fig. 10(a)), while the 50.8 GHz upconverted spectrums allows the RIN to increase only several dB (Fig. 10(b)). At an optical power of −15.5 dBm, the noise floor of the IF spectrum is dominated by RIN noise, but that of the upconverted signal is dominated by the receiver noise. The HBT-OUP link suppresses the LD's RIN due to the HBT-OUP's conversion loss.

III. Application of an Optical Fiber/Radio Link to 50-GHz Band FM/QPSK-Subcarrier Transmission Using the HBT-Transducers

A. Video FM-Analog Transmission Link Configuration

In order to examine the practical availability of the HBT photodetectors, we configured the optical/millimeter-wave radio link systems shown in Figs. 11 and 13. In Fig. 11, the FM-analog link consists of a transmitter, an optical/RF transducer and a RF-receiver. The above-mentioned three types of photodetector (PIN-PD, HBT-DD, and HBT-OUP) are used for the optical/RF transducers. The first type of optical/RF transducer is composed of the HBT-DD, a LNA with a 37 dB gain and an 8.5 dB noise figure at 50.6 GHz, and a horn antenna with a gain of 24 dB (HBT-DD link). The second type of transducer is composed of the HBT-OUP, a local oscillator, a bandpass filter, the LNA, and the horn antenna (HBT-OUP link). For reference, a third type of transducer is composed of the PIN-PD, the LNA, and the horn antenna (PIN-PD link). On the other hand, the transmitter is composed of an optical source (LD), the EOM, and an FM-modulator for the HBT-DD and PIN-PD links, and the HBT-OUP link adds a down-converter to the transmitter. The RF receiver is made up of the antenna and an FM demodulator with an 18 dB noise figure. A 50.6 GHz FM signal with a maximum frequency deviation of 8 MHz, maximum modulation frequency of 8.1 MHz and a required RF bandwidth of 37 MHz, is supplied to the EOM and the down-converter. The output power of FM-modulator is 12 dBm.

B. FM Analog Video Transmission Experimental Result

These three types of links are characterized in terms of weighted SNR using an NTSC video signal generator and analyzer. The weighted SNR is first measured by direct connection of the 50 GHz FM-modulator and demodulator (Modem back-to-back), and is subsequently measured with the links inserted. The weighted SNR for these links was evaluated by varying the three parameters of received optical power, transducer transmission power, and the pass length between two antennas. The average weighted SNR of the modem back-to-back is 57 dB. Fig. 12(a) shows the received optical power dependence of the weighted SNR for three links at a radio path length of 3 m. The PIN-PD link cannot achieve a 40 dB weighted SNR, which is an optimal level for television quality. Although the two HBT links include millimeter-wave probe loss of 4.7 dB in the experimental system, the HBT-DD link and the HBT-OUP link can achieve a weighted SNR of more than 40 dB above the received average optical power of −9 dBm and −16 dBm, respectively.

Fig. 12(b) shows the transducer's transmission-power dependence of the weighted SNR for the direct detection links and the HBT-OUP link at a radio path length of 3 m under the conditions of a received average optical power of −3 dBm for the PIN-PD link and −5.5 dBm for the HBT-DD link. A lower limit of the transmission power depends on the noise figure of the millimeter-wave receiver. However, the curve for the HBT-OUP link shows a tendency to suddenly decrease below the 40 dB weighted SNR, and the lower limit of the transmission power is different from that of the HBT-DD link. This is because the lower limit of the transmission power for the HBT-OUP link is affected by the LD's RIN at a received optical power of −5.5 dBm (Figs. 9 and 10).

Fig. 12(c) shows the weighted SNR versus the radio path length between two antennas at a received average optical power of −5.5 dBm for the HBT links. The transducer transmission power radiated from the LNA in the HBT-OUP link, HBT-DD link and PIN-PD link are −20 dBm, −33 dBm, and −46 dBm (i.e., their equivalent isotropically radiated

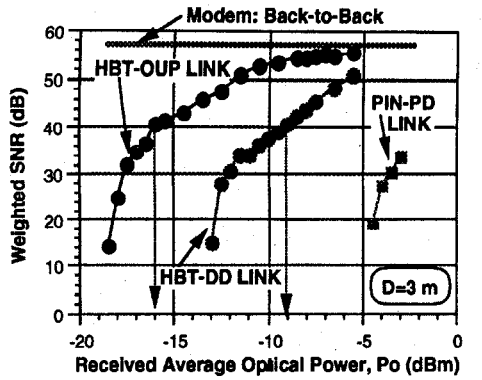

(a)

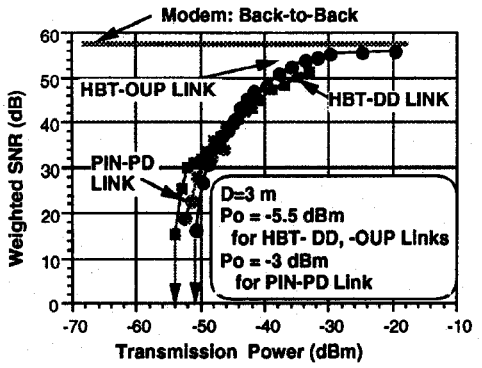

(b)

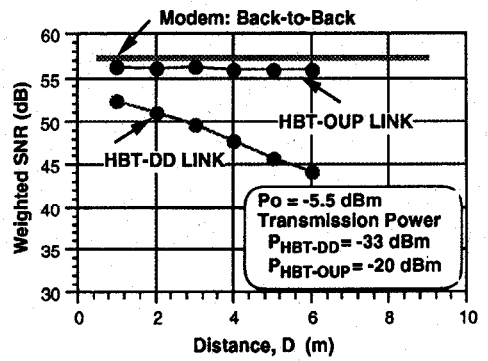

(c)

Fig. 12. Experimental results of FM-video millimeter-wave transmission link: (a) received average optical power dependence of weighted SNR at a radio path length of 3 m, (b) optical/RF-transducer transmission power dependence of weighted SNR at a radio path length of 3 m under conditions of received optical power of -3 dBm for PIN-PD link and that of -5.5 dBm for HBT links, and (c) radio path length dependence of weighted SNR at a received optical power of -5.5 dBm.

powers are 4 dBm, -9 dBm, and -22 dBm), respectively. The input-power to the EOM is 12 dBm for the direct detection (HBT-DD and PIN-PD) links and 5 dBm for the HBT-OUP link. However, the transducer transmission power from the antenna of the HBT-OUP link is higher than that of the HBT-DD or PIN-PD link. This is attributed to the low optical link loss of the HBT-OUP mentioned below. The HBT-DD link can obtain a 44 dB weighted SNR at a radio path length of 6 m indoors, and the HBT-OUP link in particular is able to achieve a 56 dB weighted SNR, which is nearly the same as that of the modem back-to-back.

The optical link losses for the PIN-PD, HBT-DD, and HBT-OUP links are 92 dB, 76 dB, and 58 dB, respectively, at the optical power of -5.5 dBm; transducer gains G_{s1} for the PIN-PD, HBT-DD, and HBT-OUP links are about 37 dB due to the RF amplifier. As a result, the transducer gain G_{s1} is smaller than the optical link loss L_{opt}. From (1), the $(G_{s1}/L_{opt}) < 1$, so the total noise figure F_t of the optical/radio link depends on each of the losses and noise figures (L_{opt},, F_{s1}, L_{radio}, F_{s2}). To realize $(G_{s1}/L_{opt}) > 1$, the direct detection (PIN-PD and HBT-DD) links need to decrease the optical link loss by using an EOM with a 3 dB-bandwidth millimeter-wave region and to increase the transducer gain through use of a high power RF amplifier. However, the HBT-OUP only requires the high power RF amplifier of more than 0 dBm output power.

C. 140 Mbps Digital Link Configuration

The 140 Mbps digital radio transmission experiment over optical fiber was made using a HBT-DD heterodyne transducer composed of the HBT-DD, an IF-amplifier, a mixer, an RF-filter, and an RF-amplifier (Fig. 13). The link consists of three sections: the QPSK modem, optical transmission and radio transmission. In this experiment, we used one of two input ports of the QPSK modulator as the clock transmission port. The NRZ bit stream (140 Mbps) and clock signal (140 MHz), filtered with low-pass filters having a 3-dB bandwidth of 117 MHz and a roll-off factor of 0.44, entered the modulator through the in-phase (I) and quadrature (Q) ports, respectively. Instead of the EOM, direct modulation of the LD is used to decrease the RIN. The QPSK signal with 2.6 GHz carrier of 9.5 dBm average power was fed into the LD intensity modulator. This heterodyne transducer detects an IF carrier of 2.6 GHz, amplifies it, upconverts it to a millimeter-wave carrier, also amplifies its millimeter-wave carrier and radiates it from the horn antenna with gain of 24 dB.

D. Digital Transmission Experimental Result

Fig. 14 shows bit error rate (BER) performance of the 140 Mbps digital transmission link using the HBT-DD heterodyne transducer. The calculated curve, which has (sub)carrier-to-noise ratio (CNR) of 19 dB at an error rate of 10^{-9}, is plotted by taking into account only the millimeter-wave receiver noise figure of 13 dB. The CNR = 19 dB are required for QPSK transmission including a 3 dB margin for fixed degradation of the modem parts. The difference of 8 dB between the calculated and measured values is assumed to be due to the RIN of laser diode, nonlinear distortion of the mixer (upconverter) in the transducer, and the HBT transducer noise. The HBT transducer noise has a smaller effect than the RIN of the laser diode at an optical power of -1 dBm (Fig. 9). Even if the optical power is in the low power region, which is dominated by the receiver noise, the noise performance of the HBT transducer is better than that of a PIN-PD receiver combined with a 50-Ω amplifier at IF frequency of the 2.6 GHz [23]–[25]. On the other hand, the nonlinear distortion of

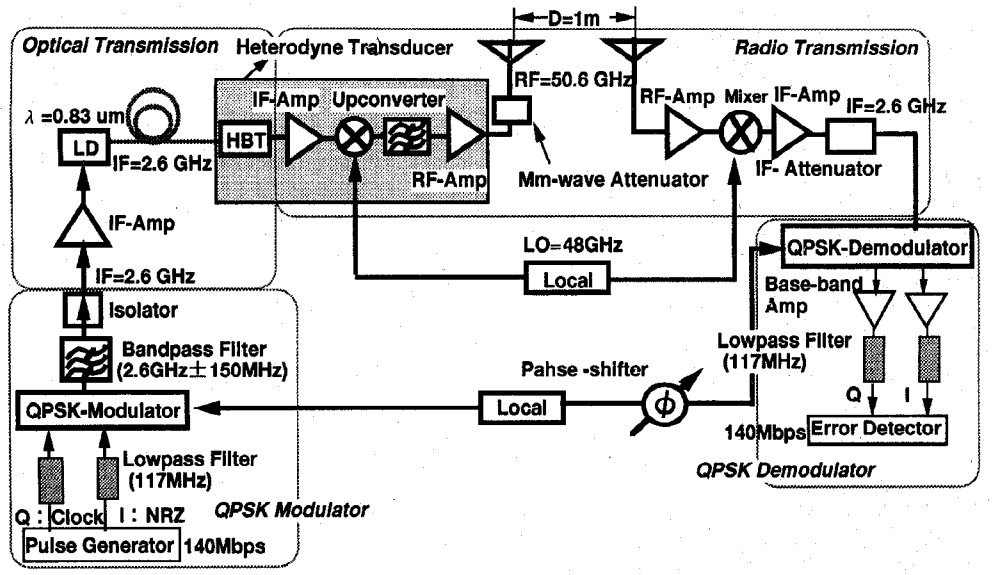

Fig. 13. Experimental configuration of 140 Mbps QPSK millimeter-wave radio transmission link using HBT-DD heterodyne transducer with external upconverter.

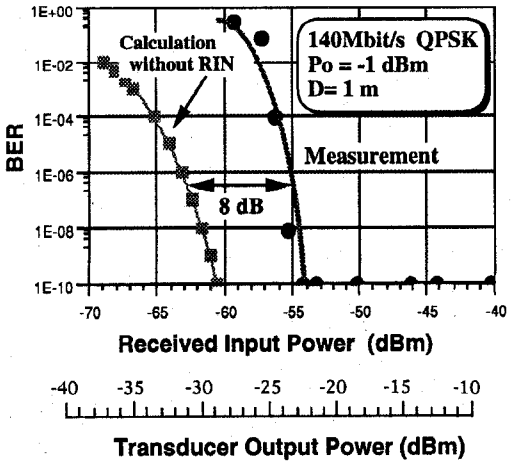

Fig. 14. BER versus HBT optical/RF transducer output power, and received input power into millimeter-wave receiver.

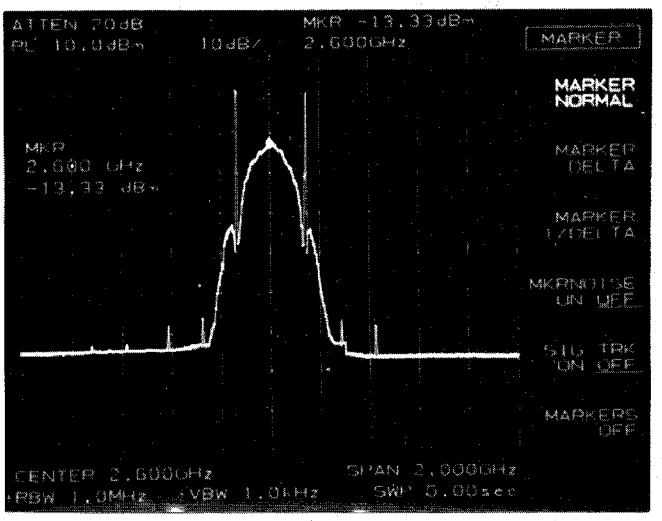

(a)

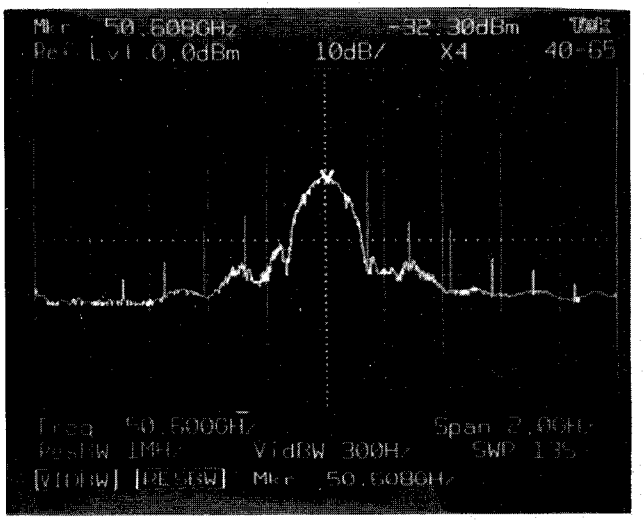

(b)

Fig. 15. Measured QPSK-spectrum of the link at (a) EOM input and (b) HBT transducer output (RF amplifier output).

the external mixer affects the BER performance to some extent. The QPSK modulation spectrums input to the LD and the antenna in the transducer are shown Fig. 15(a) and (b), respectively. In Fig. 15(b), the optical link loss decreases the CNR of the HBT transducer's spectrum, the spectrum is also formed by the RIN dominant noise floor and is distorted by the mixer in the transducer. The eye patterns for the modem's back-to-back signal and the transmission signal of the optical/radio link are shown in Fig. 16(a) and (b). A wide opening in the eye pattern can be observed for the HBT link insertion (Fig. 16(b)). Furthermore, we confirmed that 118 Mbps digital video transmission was possible using this experimental configuration.

The optical link loss of this link using the LD direct modulation is 30 dB at optical power for -1 dBm. The link loss includes the HBT internal gain (S_{21}) of about 16 dB at 2.6 GHz. On the other hand, the IF-amplifier and RF-amplifier have a gain of 11 dB and 18 dB,

TABLE II
EXPERIMENTAL RESULTS OF OPTICAL FIBER/MM-WAVE LINKS (DT: DIRECT TRANSMISSION, HT: HETERODYNE TRANSMISSION)
* USING PIN-PD RESPONSIVITY OF 0.11 A/W AND 3-dB BANDWIDTH OF 40 GHz
** USING PIN-PD RESPONSIVITY OF 0.30 A/W AND 3-dB BANDWIDTH OF 8 GHz [24], [25]

	PIN-PD Links	HBT-DD Links	HBT-OUP Link
Optical link loss (dB) @ Optical Power = - 6.5dBm and λ =0.83 μ m using EOM	DT: High (92dB)* HT: Medium (48dB)**	DT: High-Medium (76dB) HT: Low (34dB)	Medium (58dB)
Transducer Noise Performance Dependence	Subsequent Amplifier	DT: Subsequent Amplifier HT: HBT	Subsequent Amplifier
Subcarrier-to-Noise Ratio (SNR) for 50 GHz Radio Transmission	DT: Low HT: Medium	DT: Low-Medium HT: High	Medium
Bandwidth (Frequency Flatness)	DT: Large HT: Narrow	DT: Large HT: Narrow	Large
Influence of Relative Intensity Noise (RIN)	DT: Small HT: Large	DT: Small HT: Large	Small-Medium
Transducer Complexity	DT: Medium HT: Complex	DT: Simple HT: Complex	Medium
Monolithic Integration, Size	Difficult, Large-Medium	DT: Easy , Small HT: Medium, Small	Easy, Small

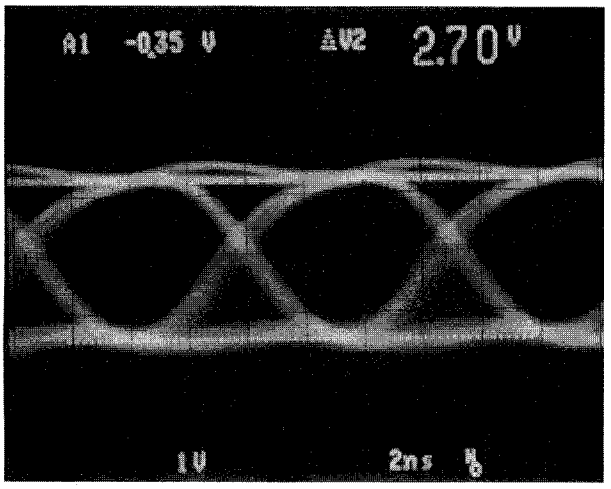

(a)

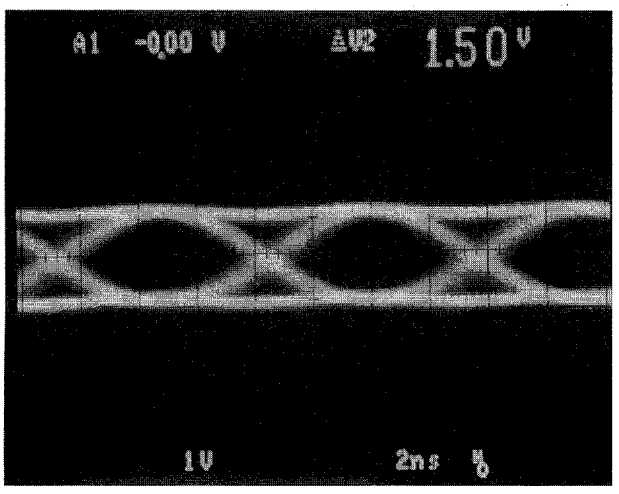

(b)

Fig. 16. Measured eye patterns of 140 Mbit/s NRZ random data stream at (a) QPSK modem back-to-back and (b) demodulator output of HBT link.

respectively. The conversion loss of the mixer including filter is about 16 dB at IF = 2.6 GHz/RF = 50.6 GHz. The total conversion gain of the transducer is estimated to be 13 dB. The poor linearity of the mixer which has 1-dB compression point of -5 dBm at IF input prevents the transducer from achieving a high gain of more than 30 dB. As a result, the transducer gain G_{s1} is smaller than the optical link loss L_{opt}. From (1), the $(G_{s1}/L_{opt}) < 1$, so the total noise figure F_t of the optical/radio link depends on each of the losses and noise figures (L_{opt}, F_{s1}, L_{radio}, F_{s2}), as with the FM-analog transmission link. However, using the high linearity mixer and IF power amplifier can give high transducer gain such that the link realizes $(G_{s1}/L_{opt}) > 1$.

IV. DISCUSSION

The feasibility of the HBT photodetectors is demonstrated in the 50 GHz band. Experimental results for the three types of HBT links: the direct transmission (DT), heterodyne transmission (HT), and optoelectronic upconversion transmission, are summarized in Table II. The direct transmission is the transmission in which both optical fiber and radio links are transmitted as millimeter-wave frequency subcarrier and carrier, respectively, while the heterodyne transmission is one in which optical fiber and radio links are transmitted as IF (microwave) frequency subcarrier and millimeter-wave frequency carrier, respectively. The heterodyne transmission for the HBT-DD link has the lowest link loss and the highest SNR of the five links because the HBT-DD has internal gain with low noise performance in the 2.6 GHz band and high optical coupling efficiency [24]–[25]. However, as for the bandwidth, the heterodyne transmission for the HBT-DD link has the narrowest bandwidth of the five links, due to IF operation of the HBT and subsequent IF amplifier and mixer. The direct transmission for the HBT-DD link is the most simple and compact configuration of the five links. The HBT-OUP link can eliminate a millimeter-wave frequency upconverter and IF amplifier.

In this paper, the HBT electrode's structure is not optimized as a photodetector. Improvements of the electrode structure and maximum oscillation frequency $f_{\max}$ for the HBT would allow responsivity of the HBT-DD and HBT-OUP to increase. In order to decrease the total noise figure F_t, the following improvements could be implemented based on (1), in order of priority: 1) the laser diode performance (optical transmitter power, linearity and RIN), and EOM bandwidth, 2) the photodetector's responsivity, the transducer noise, gain and linearity, and 3) the noise and gain of the millimeter-wave receiver terminal. The RIN is neglected in (1) in order to simplify the analysis of the optical fiber/millimeter-wave link. However, it does become an important factor for the heterodyne transmission because the relaxation oscillation frequency of the LD is nearer to the IF frequency band than the millimeter-wave band (Figs. 9 and 14).

V. Conclusion

Three types of the fiber optic/millimeter-wave links using HBT photodetectors are experimentally investigated by comparing their performances with those of the other MMIC compatible photodetector and high speed PIN-PD links. Furthermore, both digital and analog optical/millimeter-wave radio systems using video FM- and a 140 Mbps QPSK-subcarrier are introduced at a wavelength of 0.83 μm and RF frequency of 50 GHz band. We showed the possibility and effectiveness of wideband transmission using an HBT optical/RF transducer in a fiber optic/millimeter-wave personal communication system.

Although the system experiments of FM video and 140 Mbps digital transmission involve short path-length transmission of meter order in the transducer transmission power level of -20 dBm to -40 dBm, the links are promising for indoor applications (LAN and Personal Communication System) by incorporating millimeter-wave high power amplifier into the transducers and/or by using the above mentioned improvements. The MMIC HBT transducer make it possible to use the fiber optic/millimeter-wave transmission system to construct a simple and compact broadband system. Moreover, applying an InP/InGaAs HBT MMIC in the 1.3 μm- and 1.55 μm-wavelength band, would make it possible to the realize long distance, low loss transmission for personal radio communication (Fig. 1).

Acknowledgment

The authors would like to thank Dr. K. Habara, Dr. H. Inomata, and Dr. E. Ogawa of ATR Optical and Radio. Communications Research Laboratory, and Dr. H. Ogawa of NTT Wireless Systems Laboratory for their continuous support and encouragement. They would also like to thank SHARP Corp. for providing the HBT samples.

References

[1] Y. Takimoto and T. Ihara, "Research activities on millimeter wave indoor communication systems in Japan," in *IEEE MTT-S Int. Microwave Symp. Dig.*, June 1993, pp. 673–676.

[2] A. Plattner, N. Prediger, and W. Herzig, "Indoor and outdoor propagation measurements at 5 and 60 GHz radio LAN application," in *IEEE MTT-S Int. Microwave Symp. Dig.*, June 1993, pp. 853–856.

[3] R. Olshansky, V.A. Lanzisera, and P.M. Hill, "Subcarrier multiplexed lightwave systems for broad-band distribution," *J. Lightwave Technol.*, vol. 7, pp. 1329–1341, 1989.

[4] W. I. Way, "Subcarrier multiplexed lightwave system design considerations for subscriber loop applications," *J. Lightwave Technol.*, vol. 7, pp. 1806–1818, 1989.

[5] H. Ogawa, D. Polifko, and S. Banba, "Millimeter-wave fiber optics systems for personal radio communication," *IEEE Trans. Microwave Theory Tech.*, vol. 40, pp. 2285–2293, Dec. 1992.

[6] H. Ogawa and D. Polifko, "Fiber optic millimeter-wave subcarrier transmission links for personal radio communication systems," in *IEEE MTT-S Int. Microwave Conf. Dig.*, June 1992, pp. 555–558.

[7] D. Wake, N.G. Walker, and I.C. Smith, "A fiber-fed millimeter-wave radio transmitter with zero electrical power requirement," in *Proc. 23rd. European Microwave Conf.*, Sept. 1993, pp. 116–118.

[8] H. Thomas and H. Ogawa, "Indoor millimeter wave PCN/LAN experiment based on direct MMW distribution over optical fiber and multipath robust spread spectrum modulation," in *Proc. 43th IEEE Vehicular Technol. Conf.*, May 1993, pp. 236–240.

[9] H. Yano, G. Sasaki, M. Murata, and H. Hayashi, "An ultra-high speed optoelectronic integrated receiver for fiber-optic communications," *IEEE Trans. Electron Devices*, vol. 39, pp. 2254–2259, 1992.

[10] Y. Akatsu, Y. Miyagawa, Y. Miyamoto, Y. Kobayashi, and Y. Akahori, "A 10 Gb/s high sensitivity, monolithically integrated p-i-n-HEMT optical receiver," *IEEE Photon. Technol. Lett.*, vol. 5, pp. 163–165, 1993.

[11] J. B. D Soole and H. Schumacher, "InGaAs metal-semiconductor-metal photodetectors for long wavelength optical communications," *IEEE Quantum Electron.*, vol. 27, pp. 737–752, 1991.

[12] B. J. Van Zeghbroeck, W. Patrick, J. M. Halbout, and P. Vettiger, "105 GHz bandwidth metal-semiconductor-metal photodiode," *IEEE Electron Device Lett.*, vol. 9, pp. 527–529, 1988.

[13] J. C. Campbell and K. Ogawa, "Heterojunction phototransistors for long-wavelength optical receivers," *J. Appl. Phys.*, vol. 53, pp. 1203–1208, 1982.

[14] S. Chandrasekhar, M. K. Hoppe, A. G. Dentai, C. H. Joyner, and G. J. Qua, "Demonstration of enhanced performance of an InP/InGaAs heterojunction phototransistor with a base terminal," *IEEE Electron Device Lett.*, vol. 12, pp. 550–552, 1991.

[15] Y.-K. Chen, R. N. Nottenburg, M. B. Panish, R. A. Hamm, and D. A. Humphrey, "Subpicosecond InP/InGaAs heterostructure bipolar transistors," *IEEE Electron Device Lett.*, vol. 10, pp. 267–269, 1989.

[16] F. Ali and A. Gupta, *HEMT's and HBTs: Devices, Fabrication, and Circuits*. Boston: Artech House, 1991.

[17] A. Paolella, P. R. Herczfeld, A. Madjar, and T. Higgins, "Optical response of the GaAs MES FET at microwave frequencies and applications," in *IEEE MTT-S Int. Microwave Symp. Dig.*, 1991, pp. 487–490.

[18] A. Madjar, P. R. Herczfeld, and A. Paolella, "Analytical model for optically generated currents in GaAs MES FET's," *IEEE Trans. Microwave Theory Tech.*, vol. 40, pp. 1681–1691, 1992.

[19] S. Malone, A. Paolella, P. R. Herczfeld, and T. Berceli, "MMIC compatible lightwave-microwave mixing techniques," in *IEEE MTT-S Int. Microwave Symp. Dig.*, 1992, pp. 757–760.

[20] A. A. De Salles and M. A. Romero, "$Al_{0.3}Ga_{0.7}As$/GaAs HEMT's under optical illumination," *IEEE Trans. Microwave Theory Tech.*, vol. 39, pp. 2010–2017, 1991.

[21] M. Z. Martin, F. K. Oshita, M. Matloubian, H. R. Fetterman, L. Shaw, and K. L. Tan, "High-speed optical response of pseudomorphic InGaAs high electron mobility transistors," *IEEE Photon. Technol. Lett.*, vol. 4, pp. 1012–1014, 1992.

[22] S. Banba, E. Suematsu, and H. Ogawa, "Fundamental properties of HEMT photodetectors for use in fiber optic links," in *Proc. 23rd. European Microwave Conference*, Sept. 1993, pp. 747–750.

[23] H. Ogawa, S. Banba, E. Suematsu, H. Kamitsuna, and D Polifko, "A comparison of noise performance between a PIN diode and MMIC HEMT and HBT optical receivers," in *IEEE MTT-S Int. Microwave Conf. Dig.*, June 1993, pp. 225–228.

[24] E. Suematsu and H. Ogawa, "Frequency response of HBT's as photodetectors," *IEEE Microwave Guided Wave Lett.*, vol. 3, pp. 217–218, July 1993.

[25] ——, "Noise performance of MMIC HBT's as photodetectors," in *Proc. 23rd. European Microwave Conf.*, Sept. 1993, pp. 311–313.

[26] H. Kamitsuna and H. Ogawa, "Monolithic image rejection optoelectronic up-converters that employ the MMIC process," in *IEEE Microwave and Millimeter-Wave Monolithic Circuits Symp.*, 1993, pp. 75–78.

[27] J. K. Twynam, H. Sato, and T. Kinosada, "High-performance carbon-doped base GaAs/AlGaAs heterojunction bipolar transistor grown by MOCVD," *Electron. Lett.*, vol. 27, pp. 141–142, 1991.

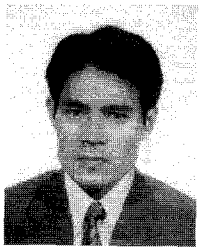

Eiji Suematsu (A'92) was born in Kumamoto, Japan in 1960. He received the B.S. and M.S. degrees in geology from Kumamoto University, Kumamoto, Japan, in 1984 and 1986, respectively.

In 1986, he joined the Central Research Laboratories of Sharp Corporation, Nara, Japan. He was engaged in research and development on low-noise FET's and MMIC's. Since 1992, he joined ATR Optical and Radio Communications research Laboratories, Kyoto, Japan where he was engaged in research of millimeter-wave fiber optic radio systems. Since 1994, he has been involved in research of millimeter-wave MMIC at the Central Research Laboratories of Sharp Corporation, Nara, Japan.

Mr. Suematsu is a member of the Institute of Electronics, Information, and Communication Engineers of Japan.

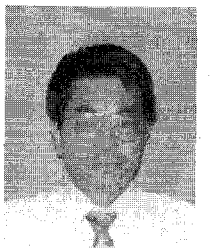

Nobuaki Imai (M'86) was born in Kochi, Japan, 1953. He received the B.S. degree in electrical engineering from Nagoya Institute of Technology, Nagoya, Japan, in 1975, and the M.S. degree from Kyoto University, Kyoto, Japan, in 1977.

He joined NTT Electrical Communication Laboratories, Yokosuka, Japan, in 1977. He has been engaged in research on microwave and millimeter-wave integrated circuits and the development of digital microwave radio systems. In 1993, he moved to ATR Optical and Radio Communications Research Laboratories and has been engaged in research on millimeter-wave fiber optic radio systems.

Mr. Imai is a member of the Institute of Electronics, Information, and Communication Engineers of Japan.